Aberrant motor axon projection, acetylcholine receptor clustering, and neurotransmission in cyclin-dependent kinase 5 null mice

Amy K. Y. Fu*†, Fanny C. F. Ip*†, Wing-Yu Fu*, Janet Cheung*, Jerry H. Wang*, Wing-Ho Yung‡, and Nancy Y. Ip*§

*Department of Biochemistry, Biotechnology Research Institute, and Molecular Neuroscience Center, The Hong Kong University of Science and Technology, Clear Water Bay, Hong Kong, China; and ‡Department of Physiology, Chinese University of Hong Kong, Shatin, Hong Kong, China

Communicated by Gerald D. Fischbach, Columbia University College of Physicians and Surgeons, New York, NY, September 2, 2005 (received for review May 17, 2005)

Cyclin-dependent kinase (Cdk)5 is a key regulator of neural development. We have previously demonstrated that Cdk5/p35 are localized to the postsynaptic muscle and are implicated in the regulation of neuregulin/ErbB signaling in myotube culture. To further elucidate whether Cdk5 activity contributes to neuromuscular junction (NMJ) development *in vivo*, the NMJ of Cdk5$^{-/-}$ mice was examined. Consistent with our previous demonstration that Cdk5 phosphorylates ErbB2/3 to regulate its tyrosine phosphorylation, we report here that the phosphorylation of ErbB2 and ErbB3 and the ErbB2 kinase activity are reduced in Cdk5-deficient muscle. In addition, Cdk5$^{-/-}$ mice also display morphological abnormalities at the NMJ pre- and postsynaptically. Whereas the outgrowth of the main nerve trunk is grossly normal, the intramuscular nerve projections exhibit profuse and anomalous branching patterns in the Cdk5$^{-/-}$ embryos. The central band of acetylcholine receptor (AChR) clusters is also wider in Cdk5$^{-/-}$ diaphragms, together with the absence of S100 immunoreactivity along the phrenic nerve during late embryonic stages. Moreover, we unexpectedly discovered that the agrin-induced formation of large AChR clusters is significantly increased in primary muscle cultures prepared from Cdk5-null mice and in C2C12 myotubes when Cdk5 activity was suppressed. These abnormalities are accompanied by elevated frequency of miniature endplate potentials in Cdk5-null diaphragm. Taken together, our findings reveal the essential role of Cdk5 in regulating the development of motor axons and neuromuscular synapses *in vivo*.

agrin | Cdk5 | ErbB receptor | neuromuscular junction

Cyclin-dependent kinase (Cdk)5, a Pro-directed Ser/Thr Cdk, has been identified as a key regulator in neural development. Distinct from other Cdks, Cdk5 is not involved in cell-cycle control, and its activation requires the recruitment of neuron-specific activators p35 or p39 (1). Much of our understanding on the involvement of Cdk5 in neuronal positioning is derived from gene-targeting studies. Cdk5$^{-/-}$ mice exhibit widespread disruption of normal lamination in brain regions (2), and similar cortical lamination disruption has also been reported in the p35$^{-/-}$ mice (3). Furthermore, the defects observed in the fasciculation of axon tracts in p35$^{-/-}$ mice suggest that Cdk5 is also involved in axon patterning (4).

In addition to gene-targeting studies, identification of the repertoire of Cdk5 protein substrates revealed that this multifaceted kinase is also involved in other key functions in the nervous system, including neurite outgrowth, axon guidance, and neuronal survival (1). The localization of Cdk5/p35 to synapses and identification of various substrates at both pre- and postsynaptic terminals suggest that Cdk5 may play a functional role in synapse formation (5–8). The neuromuscular junction (NMJ) has served as an excellent model for explicating the pathways implicated in synapse formation. Formation of the NMJ requires precise and coordinated interactions among motor nerve terminals, Schwann cells, and muscle fibers (9). NMJ formation is marked by the clustering of acetylcholine receptors (AChRs) followed by the stabilization of AChR clusters and the formation of endplate band at embryonic day (E)18.5. Two key signaling pathways involving receptor tyrosine kinases, muscle-specific kinase (MuSK) and ErbB receptors, emerge as prominent players in postsynaptic differentiation at the NMJ (10). Agrin, released by motor neurons, binds to the MuSK-receptor complex and activates its downstream signaling cascade in muscle, leading to the clustering of AChRs (11). Activation of ErbB, on the other hand, requires neuregulin-1 (NRG) (also known as ARIA), a member of a family of growth factors produced by alternative splicing of the *nrg-1* gene (12). NRG binds to ErbB receptors and, through the initiation of Erk signaling pathway, induces the transcription of synapse-specific genes, such as AChR subunits (13). Nonetheless, recent studies indicate that, although conditional mutant mice lacking NRG or ErbB receptors exhibit neuromuscular defects, the pattern of AChR transcription remains grossly normal in these mice (14–16).

We have previously reported that Cdk5/p35 is localized to the adult NMJ and is involved in regulating NRG-activated downstream signaling in myotube culture (5). To assess the roles of Cdk5 in synapse formation *in vivo*, we examined the development of NMJ in mice lacking Cdk5. In particular, we focused on examining the diaphragm muscle, where synaptogenesis has been well characterized (17). Our analysis shows that there are pre- and postsynaptic defects at the developing NMJ in Cdk5-deficient embryos, thus revealing an important role of Cdk5 in the formation of peripheral synapses.

Materials and Methods

Chemicals and Antibodies. Abs specific for p35 (c-19), Cdk5 (c-8), ErbB2 (c-18), ErbB3 (c-17), Akt (N19), and utrophin (c19), were purchased from Santa Cruz Biotechnology. Phospho-Akt Ab was purchased from Cell Signaling Technology (Beverly, MA), phospho-Tyr Ab (4G10) from Upstate Biotechnology (Lake Placid, NY), and Abs specific for neurofilament (NF)150 and phospho-Ser and phospho-Thr residues were from Chemicon, synaptophysin from Zymed, S100 from DAKO, and SV2 from Developmental Studies Hybridoma Bank (University of Iowa, Iowa City, IA). The FITC-conjugated goat anti-rabbit Ab was purchased from ICN and rhodamine-conjugated α-bungarotoxin (αBTX) from Molecular Probes. Agrin was purchased from R & D Systems, and roscovitine (Ros) from Calbiochem.

Abbreviations: AChR, acetylcholine receptor; Cdk, cyclin-dependent kinase; E, embryonic day; MEPP, miniature end-plate potential; MuSK, muscle-specific kinase; NF, neurofilament; NMJ, neuromuscular junction; NRG, neuregulin-1; Ros, roscovitine; siRNA, small interfering RNA.

†A.K.Y.F. and F.C.F.I. contributed equally to this work.

§To whom correspondence should be addressed at: Department of Biochemistry, Hong Kong University of Science and Technology, Clear Water Bay, Hong Kong, China. E-mail: boip@ust.hk.

www.pnas.org/cgi/doi/10.1073/pnas.0507678102

Cell Culture, Transfection, and AChR Clustering. Cdk5 knockout embryos were collected and genotyped as described in ref. 2. Primary muscle culture from Cdk5$^{-/-}$ embryos and mouse C2C12 cells were prepared and maintained as described in ref. 5. A Cdk5 inhibitor, Ros (5), was added to the myotube culture before agrin (5 ng/ml) or NRG (3 nM) treatment. Schwann cells were purified from the sciatic nerve of postnatal day 1 rats, as described in ref. 18. For survival assay, the cells were fixed and labeled by using TUNEL assay (Promega) and Hoechst 33342 (Sigma), as described in ref. 19. Chemically modified small interfering RNA (siRNA)-targeting Cdk5 was designed and synthesized according to the manufacturer's instruction by using the Stealth RNA interference technology (Invitrogen). Differentiated C2C12 myotubes were transfected with Cdk5 siRNA by using Lipofectamine 2000 (Invitrogen).

Primary muscle and C2C12 myotube cultures were treated with recombinant agrin for 16 and 8 h, respectively. Myotubes were stained by using αBTX, and the AChR clusters from $\approx$20 random fields per dish were imaged by using a confocal microscope for primary muscle culture and fluorescent microscopy (Leica) for C2C12 myotubes (n = 3 dishes). The area of AChR clusters was measured by using Metamorph IMAGE ANALYSIS software (Universal Imaging, Downingtown, PA).

Northern Blot, Real-Time PCR Analysis, and Whole-Mount *in Situ* Hybridization. Total RNAs of mouse tissues were prepared by lithium chloride/urea extraction, and Northern blot analysis was performed as described in ref. 20. Total RNA of Schwann cells was collected, reverse transcribed, and used for real-time PCR analysis according to the manufacturer's instruction. The identity of PCR products was confirmed by Southern blot analysis. For whole-mount *in situ* hybridization, a digoxigenin-labeled cRNA probe specific for mouse AChRα subunit was transcribed *in vitro*, and hybridization was performed as described in ref. 21.

Immunohistochemical Analysis, Immunoprecipitation, and Kinase Assays. For immunohistochemical analysis, diaphragm muscles from E15.5 to E18.5 embryos were dissected, fixed, and stained with Abs against NF150 (1:500), synaptophysin (1:100), or S100 (1:100), followed by FITC-conjugated goat anti-rabbit Ab and αBTX (22). Z-serial images were collected with confocal microscopy (BX61, Olympus). The images presented represent single-projected images derived from overlaying each set of Z-images.

Limb muscles from E18.5 embryos were collected for ErbB phosphorylation and kinase assays as described in refs. 5 and 23. Detection of p35-associated Cdk5 kinase activity in Schwann cells was performed as described in ref. 5.

Electrophysiology. The intact diaphragms with attached phrenic nerves were dissected from E18 embryos and placed in oxygenated NMR solution. The resting membrane potential and spontaneous miniature end-plate potentials (MEPPs) were recorded by a microelectrode amplifier (Axoclamp 2B, Axon Instruments). The ability of phrenic nerve to conduct electrical signals was tested by stimulating the nerve supramaximally via a suction electrode connected to a stimulus isolation unit (Digitimer, DS-2). At the end of experiment, the presence of functional AChRs was tested by bath application of the agonist carbachol (50 μM). Data were collected and analyzed by PCLAMP (ver. 7, Axon Instruments, Union City, CA) and MINIANALYSIS (ver. 5.1, Synaptosoft, Decatur, GA).

Data Analysis and Statistics. Immunoblots were scanned, and the band intensity was quantified by using IMAGE J software (National Institutes of Health, Bethesda). The width of AChR endplate zone, area of AChR clusters, and axon length were quantified by using Metamorph IMAGE ANALYSIS software (Universal Imaging). The width of AChR endplate zone in the diaphragm was measured as previously described; n = 24 per images from three diaphragms (24). The average axon length was quantified by measuring the average axon length extended from the main nerve trunk. The statistical significance of the quantitative analysis was determined by using the unpaired Student t test. The MEPPs were analyzed with the aid of MINIANALYSIS software and compared by using the one-way ANOVA followed by the Tukey test.

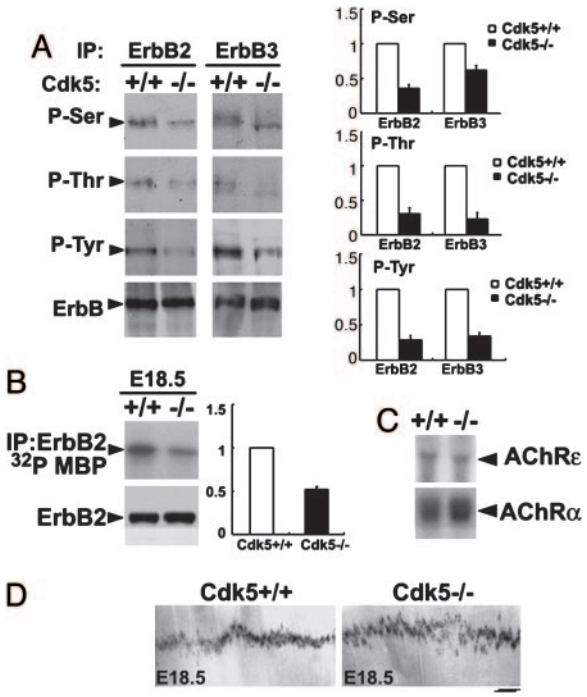

Fig. 1. Attenuation of ErbB2/3 phosphorylation and ErbB2 kinase activity in Cdk5$^{-/-}$ muscle and expression of AChR transcript. (*A*) Phosphorylation of ErbB2/3 on Ser, Thr, and Tyr sites (P-Ser, P-Thr and P-Tyr) and total ErbB2/3 protein in limb muscle of WT and Cdk5$^{-/-}$ E18.5 embryos. Ratio of the band intensity relative to the corresponding total ErbB expression (*Right*). (*B*) ErbB2 kinase activity and total ErbB2 protein in limb muscle of WT and Cdk5$^{-/-}$ embryos at E18.5; ratio of kinase activity (*Right*). All experiments have been repeated three times. (*C*) Northern blot analysis for AChRα and -ε subunit in limb muscle of WT and Cdk5$^{-/-}$ embryos at E17.5. (*D*) Whole-mount *in situ* hybridization of E18.5 diaphragm prepared from WT and Cdk5$^{-/-}$ embryos by using digoxigenin-labeled cRNA probe encoding AChRα. (Scale bar, 200 μm.) Measurement of the endplate bandwidth was as described in *Materials and Methods*; n = 3 images from individual diaphragms.

Results

ErbB Receptor Phosphorylation and Activity Were Attenuated in Muscles of Cdk5$^{-/-}$ Embryos. We have previously reported that Cdk5 phosphorylates ErbB2/3 receptor at Ser and Thr residues to regulate the Tyr phosphorylation of the receptors (5, 25). Consistent with these findings, phosphorylation of ErbB2 and ErbB3 on Ser, Thr, and Tyr residues was reduced in muscle lacking Cdk5 (Fig. 1*A*). Furthermore, ErbB2 kinase activity was reduced in Cdk5$^{-/-}$ muscle by $\approx$60%, when compared with that of WT (Fig. 1*B*). Whereas the levels of AChRα and AChRε transcripts were not significantly altered in Cdk5$^{-/-}$ hindlimb muscle (Fig. 1*C*), localization of AChR clusters was slightly affected. *In situ* hybridization revealed that, although the transcript encoding the AChRα subunit was restricted to the synaptic sites and confined as a narrow band in the central region of the diaphragm for both WT and Cdk5$^{-/-}$ diaphragms, the band was slightly broader (increased by $\approx$10%) in mutant diaphragms (Fig. 1*D*). Furthermore, no obvious defects in the localization of specific pre- and postsynaptic site markers, such as SV2 and utrophin, were observed in Cdk5$^{-/-}$ limb muscle (data not shown). Thus, ErbB signaling and AChR localization are affected in Cdk5$^{-/-}$ muscles.

NEUROSCIENCE

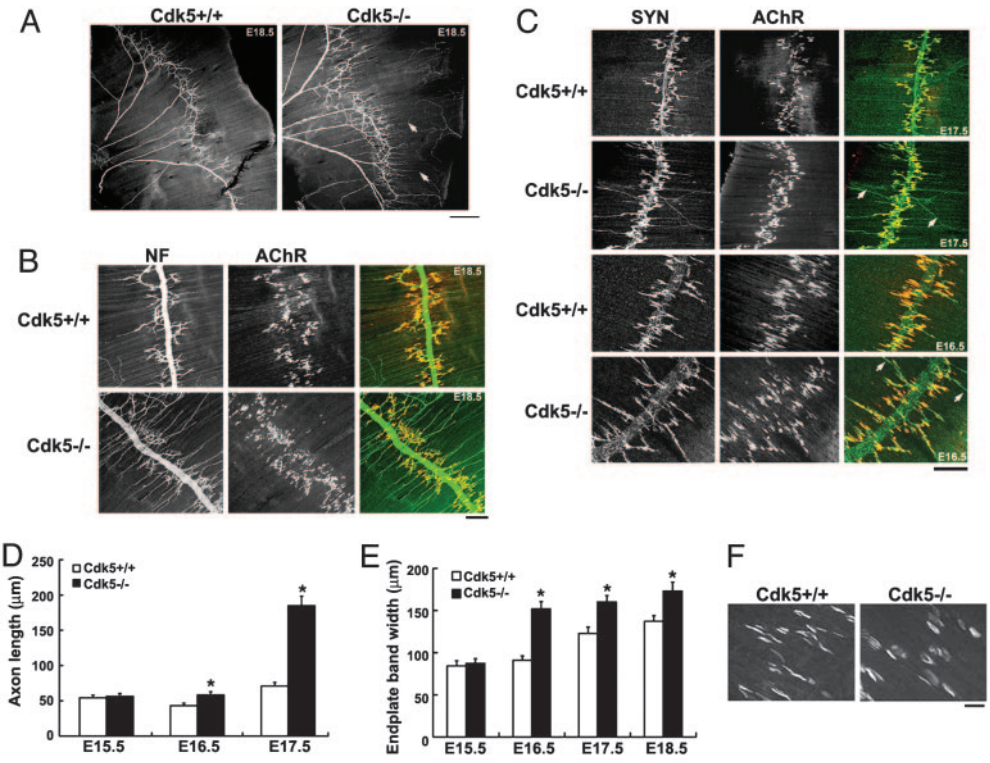

Fig. 2. Aberrant projections of motor axons with disorganized nerve terminals extending further beyond the central band of AChRs in Cdk5$^{-/-}$ diaphragm muscle. (*A*) The right halves of the whole-mount diaphragms of E18.5 Cdk5$^{+/+}$ and Cdk5$^{-/-}$ embryos stained with NF150 Ab. (Scale bar, 500 μm.) (*B*) A higher magnification showing the NF (green) and AChR staining (αBTX, red) in diaphragm muscle. Examples of aberrant axon extensions are indicated by arrows. (Scale bar, 100 μm.) (*C*) Whole-mount diaphragm muscles from E17.5 and E16.5 Cdk5$^{+/+}$ and Cdk5$^{-/-}$ embryos were stained with Ab against synaptophysin (SYN, green) to label the synaptic vesicle and with αBTX to label AChR. Examples of nerve terminals extending beyond the zone of AChR clusters in mutant diaphragm muscle are indicated by arrows. Measurement of the axon length (*D*) and width (*E*) of AChR endplate bands. (*F*) Higher magnification of AChR clusters in E18.5 diaphragm muscles.

Motor Axon Arborization and Increased Endplate Band Width in Diaphragm Muscles of Cdk5$^{-/-}$ Embryos. Newborn Cdk5$^{-/-}$ mice exhibited cyanotic condition and reduced mobility of four limbs (2). In addition, we found that the forelimbs of Cdk5$^{-/-}$ mice pointed downwards with diminished response to pinching stimuli. These observations are indicative of potential aberrant innervations at the NMJ. To determine whether the NMJ innervation was affected in Cdk5$^{-/-}$ mice, motor axon projections in diaphragm muscles of Cdk5$^{-/-}$ mice were examined. The phrenic nerves of E18.5 mice were visualized in whole-mount preparation by staining with NF Ab to label the intramuscular nerves. Remarkably, whereas the projections of motor axons terminated close to the main nerve trunk in control embryos, the motor axons of Cdk5$^{-/-}$ embryos projected aberrantly, extending much further across the diaphragm muscle [Fig. 2 *A* and *B*; 83 $\pm$ 9 μm in E18.5 WT muscle (n = 32) vs. 135 $\pm$ 11 μm in Cdk5$^{-/-}$ muscle (n = 45), $P < 0.001$]. The alignment of motor axon projections to the postsynaptic AChR endplates was further examined by visualizing presynaptic nerves with synaptophysin antibodies and AChR clusters with αBTX (Fig. 2*C*). Whereas the nerve terminals were directly juxtaposed to AChR clusters in WT diaphragm, the preterminal axons extended a long distance from both sides of the nerves, passing through and projecting beyond the central band of AChR clusters in Cdk5$^{-/-}$ diaphragm by E16.5 (Fig. 2 *C* and *D*). At E17.5, most of the nerve terminals failed to terminate at synaptic sites within the central band of AChR clusters in Cdk5$^{-/-}$ embryo (Fig. 2 *C* and *D*). In agreement with our *in situ* hybridization observation, the width of the central band of AChR clusters was broader in Cdk5$^{-/-}$ muscle (123 $\pm$ 8 μm in E17.5 WT diaphragm muscle vs. 160 $\pm$ 8 μm in Cdk5$^{-/-}$ muscle; Fig. 2*E*).

Number of Large AChR Clusters Was Increased in Primary Muscle Cultures Prepared from Cdk5$^{-/-}$ Embryos. Upon examination of AChR clusters, we observed that the size of AChR clusters in E18.5 Cdk5$^{-/-}$ diaphragm was apparently larger than that observed in the WT control (Fig. 2*F*). To verify whether the changes in AChR cluster size *in vivo* were attributable to the loss of Cdk5 activity, we first sought to determine whether Cdk5 regulates the size of agrin-induced AChR clusters in cultured myotubes. Myoblasts were isolated from WT and Cdk5$^{-/-}$ embryos. Formation of myotubes was seemingly unaffected in the absence of Cdk5 activity. Before agrin treatment, very few AChR clusters were detected in both control and Cdk5$^{-/-}$ myotube cultures (data not shown). Treatment with agrin induced the formation of large AChR clusters (>200 pixels) and small clusters (25–100 pixels) in cultured WT myotubes. Interestingly, the absence of Cdk5 activity altered the relative abundance of large and small clusters, where a significant increase in the number of large clusters and a reduction in small clusters were observed (Fig. 3 *A* and *B*). To further elucidate the role of Cdk5 in AChR cluster size, we examined the effect of suppressing Cdk5 activity on agrin-induced AChR clusters in C2C12 myotubes. Treatment with Cdk5 inhibitor Ros before agrin treatment significantly increased the number of agrin-induced large AChR clusters (>150 pixels; Fig. 3 *C* and *D*). Similarly, the number of agrin-induced AChR clusters was increased in myotubes transfected with Cdk5 siRNA (Fig. 3 *E–H*). These observations suggest that the number and size of AChR clusters were enhanced when Cdk5 activity was attenuated. Finally, the effect of Cdk5 activity on the signaling implicated in agrin-induced clustering of AChR was examined. Agrin induces AChR clustering through the activation of Rho small GTPases and Pak (26, 27). Interestingly, we found that blockade of Cdk5 expression also affected agrin-induced Pak phosphorylation and activity (data not shown).

Lack of S100-Immunoreactivity Along Phrenic Nerves in Cdk5$^{-/-}$ Embryos. NRG signaling is a key regulator of Schwann cell survival during the early stages of development via the PI3K/Akt pathway (28, 29). Given our observation that Cdk5 affects NRG/ErbB signaling (5), we were interested to examine whether the integrity of Schwann cells, an integral component of the NMJ, was affected in Cdk5$^{-/-}$ embryos. Schwann cells in phrenic nerves were visualized by staining against S100 Ab. Whereas S100 staining accompanying the entire phrenic nerve could be observed in Cdk5$^{-/-}$ embryos at E15.5 (Fig. 4*A*), it was absent at E17.5 and E18.5 (Fig.

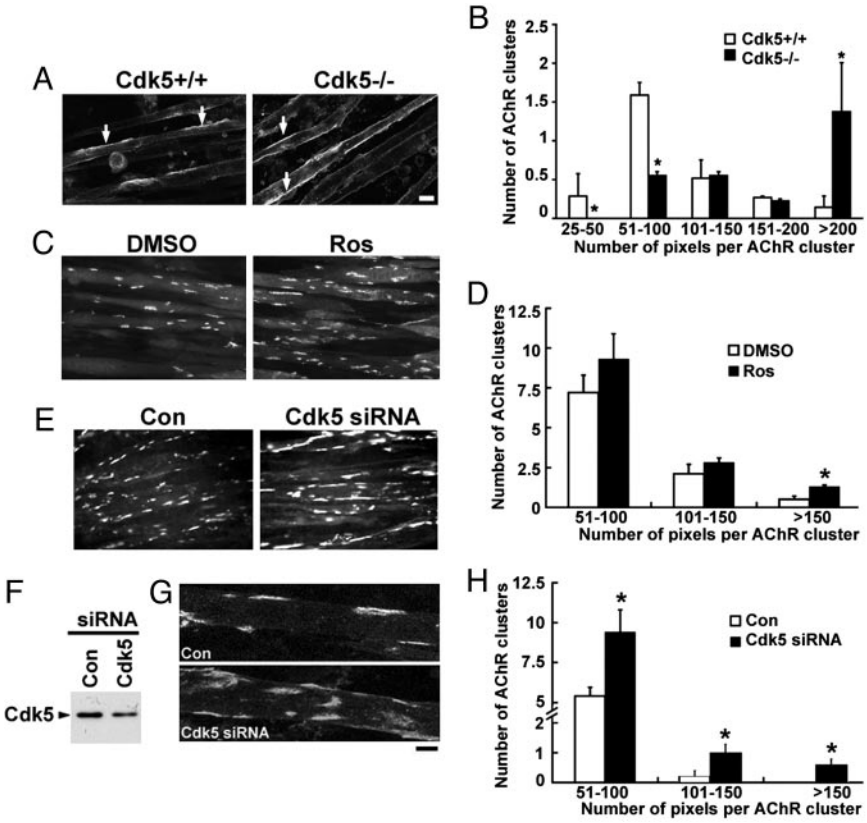

Fig. 3. Cdk5 activity regulated the size of agrin-induced AChR clusters in cultured myotubes. (*A*) Alteration in size distribution of agrin-induced AChR clusters in cultured myotubes prepared from $Cdk5^{-/-}$ mice. Myotube cultures prepared from $Cdk5^{+/+}$ and $Cdk5^{-/-}$ E18.5 embryos were treated with recombinant agrin for 16 h and stained with αBTX (AChR). (Scale bar, 10 μm.) Examples of AChR clusters are indicated with arrows. (*B*) Morphometric analysis of AChR clusters in primary muscle cultures. The length of AChR clusters was quantified by METAMORPH and arbitrarily assigned as number of pixels. Values represent mean ($\pm$SEM); $*$, $P < 0.005$. (*C*) C2C12 myotubes were pretreated with DMSO or Ros for 4 h, followed by agrin treatment for 16 h, and were fixed and stained for AChR clusters. (*D*) Morphometric analysis of agrin-induced AChR clusters in cultured C2C12 myotubes without (DMSO) or with (Ros) pretreatment. Values represent mean ($\pm$SEM); $*$, $P < 0.005$, when compared with DMSO pretreatment. (*E*) C2C12 myotubes transfected with Cdk5 siRNA or scramble siRNA were treated with agrin for 8 h and stained with αBTX. The reduction of Cdk5 expression in Cdk5 siRNA-transfected C2C12 myotubes was depicted in *F*. (*G*) Single-projected images of a set of Z-images (5 μm, at 1-μm intervals) obtained by confocal microscope. (Scale bar, 10 μm.) (*H*) Morphometric analysis of AChR clusters in C2C12 myotubes transfected with Cdk5 siRNA. Values represent mean ($\pm$SEM); $*$, $P < 0.005$, when compared with that transfected with scramble siRNA.

4 *B–D*). Interestingly, the terminal Schwann cells remained intact in $Cdk5^{-/-}$ embryos at both E17.5 and E18.5 stages (Fig. 4 *B–D*). To verify whether the loss of S100 staining in $Cdk5^{-/-}$ embryos was, at least in part, attributable to the absence of Cdk5 activity in Schwann cells, we first examined whether active Cdk5 is present in cultured Schwann cells. We found that low levels of p35 mRNA- and p35-associated Cdk5 activity could be detected in enriched Schwann cell culture (Fig. 4 *E* and *F*). Because the decrease in S100 staining observed in mutant embryos could be due to the absence of S100 protein or loss of Schwann cells, the consequence of inhibiting Cdk5 activity on NRG-mediated Akt signaling and cell viability in cultured Schwann cells was investigated. Consistent with an earlier report (30), NRG treatment induced the phosphorylation of Akt in these cells within 5 min (Fig. 4*G*). Inhibition of Cdk5 activity by Ros (5) attenuated the NRG-induced phospho-Akt ($50 \pm 3\%$). More importantly, whereas a significant increase in the survival of serum-deprived Schwann cells was observed in response to NRG treatment (>93%), this effect was attenuated in the presence of Ros (Fig. 4*H*), suggesting that the lack of S100 staining in $Cdk5^{-/-}$ phrenic nerves was likely due to the loss of Schwann cells. Interestingly, the morphology and functions of these Schwann cells and their expression profiles of ErbB receptors are quite different from terminal Schwann cells (18, 28, 31). It is possible that the absence of defects in terminal Schwann cells of $Cdk5^{-/-}$ embryos is, in part, because of their differential requirement of NRG/ErbB signaling.

Neurotransmission Was Increased in Diaphragm Muscles of $Cdk5^{-/-}$ Embryos. To examine whether the pre- and postsynaptic abnormalities observed in $Cdk5^{-/-}$ mice affect synaptic transmission, intracellular recording of diaphragm muscle was performed. The majority of muscle fibers, irrespective of their genotypes, exhibited spontaneous MEPPs, either at rest or upon challenge by a high concentration of K^+. Moreover, application of carbachol caused massive contraction of all preparations tested (data not shown). These observations indicate that mutant muscles had functional AChRs, which responded to quantal release of acetylcholine from nerve terminals. However, $Cdk5^{-/-}$ muscles exhibited significantly higher frequencies of MEPPs, either at rest or after depolarization with 40 mM K^+ (Fig. 5 *B* and *D*). These findings suggest that presynaptic terminal functions at the NMJs were defective in mutant embryos, with an increase in spontaneous neurotransmitter release. Importantly, postsynaptic abnormality was also evident in $Cdk5^{-/-}$ muscles, whereby they tended to receive bursts of synaptic activities upon challenge with 40 mM K^+ (Fig. 5*C*). Furthermore, distinctive types of MEPPs in some $Cdk5^{-/-}$ muscles suggest that these muscles had motor endplates that were spatially far apart (Fig. 5*C*). Because the recording electrodes were routinely placed in the central band of muscles, the slower MEPPs probably originated from more peripheral regions.

Discussion

We describe in this study that $Cdk5^{-/-}$ mice exhibit pre- and postsynaptic defects at the developing NMJ, supporting an important role of Cdk5 in NMJ development. In $Cdk5^{-/-}$ mice, defects were found at motor nerve terminals, Schwann cells, and muscle fibers. Projections of peripheral motor nerves exhibit aberrant branching patterns, with preterminal axons passing through the central band of AChRs in muscle. Loss of S100 protein along the phrenic nerve, broadening of the AChR endplate band, and changes in the size of AChR clusters in muscle were also detected. Finally, our electrophysiological studies reveal an important function of Cdk5 in regulating synaptic transmission, consistent with the role of Cdk5 in transmitter release and postsynaptic specializations.

It is noteworthy that the NMJ phenotype of $Cdk5^{-/-}$ embryos reported here is, in some ways, similar to that of mutant mice lacking NRG or ErbB receptors (14). Mice with defective NRG/ErbB signaling exhibit severe neuromuscular defects, including abnormal outgrowth and aberrant projections of phrenic nerves,

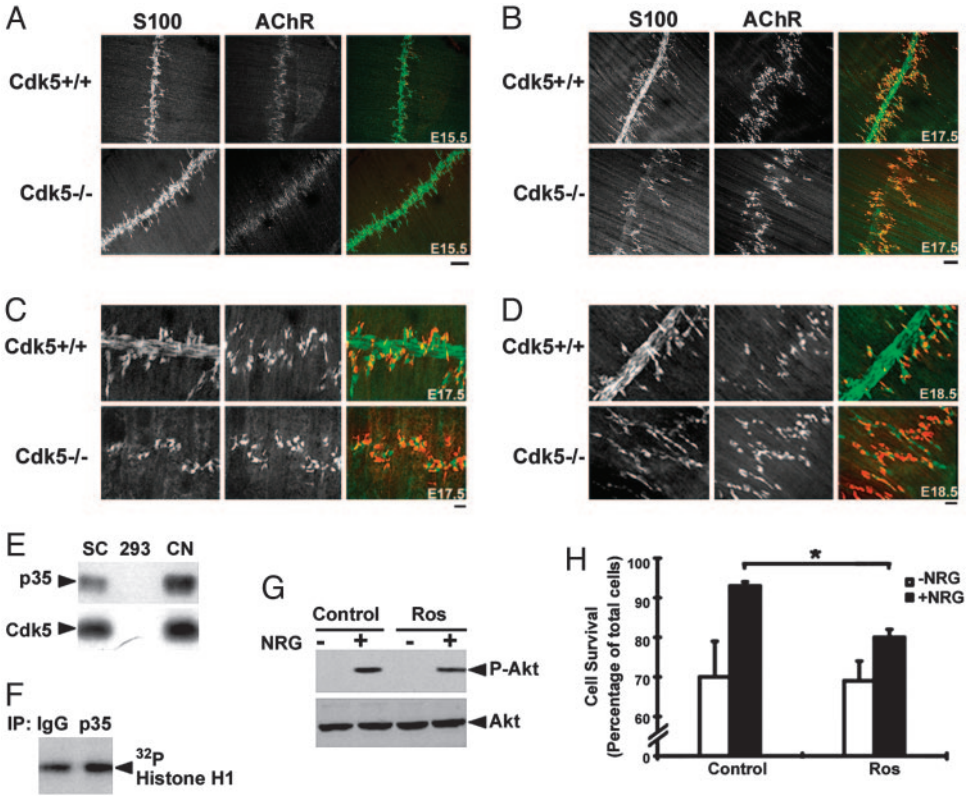

Fig. 4. Absence of S100 staining in the phrenic nerves of diaphragms from E17.5 and E18.5 Cdk5$^{-/-}$ embryos. Diaphragm muscle from Cdk5$^{+/+}$ and Cdk5$^{-/-}$ embryos at E15.5 (*A*), E17.5 (*B* and higher magnification in *C*), and E18.5 (*D*) were stained with S100 Ab (green) and αBTX (AChR, red). (Scale bar, 100 μm in *A* and *B*.) (Scale bar, 20 μm in *C* and *D*.) (*E*) p35 and Cdk5 mRNA expression in Schwann cell culture. SC, day 10 Schwann cell culture; HEK-293, human embryonic kidney cell line; CN, day 21 cortical neuron culture. (*F*) p35-associated Cdk5 kinase activity in Schwann cell culture. (*G*) Reduction of Akt phosphorylation in Ros-treated Schwann cells. At 24 h after replating, Schwann cells were preincubated with or without Ros (40 μM) for 1 h, followed by treatment with NRG (+) at 37°C for 5 min. Western blot analysis for phospho-Akt (P-Akt) and total Akt. (*H*) Inhibition of NRG-mediated Schwann cell survival by Ros. Schwann cells were maintained in serum-free medium with or without NRG in the presence or absence of Ros (10 μM). Cell survival was assessed by using Hoechst dye and TUNEL assay (data not shown). The number of viable cells was counted, and cell survival was expressed as a percentage of the total number of cells. Values represent mean (±SEM), $n = 3$; *, $P < 0.005$ for NRG-induced cell survival in the presence or absence of Ros.

absence of Schwann cells, and eventual degeneration of motor nerves. Whereas the NMJ phenotype of the Cdk5$^{-/-}$ embryos is less severe than those reported for NRG/ErbB mutant mice, the exuberant growth of motor axons is similarly observed. In addition, AChR endplate bands of diaphragm muscle remain largely unchanged or broadened in NRG/ErbB-mutant mice (32, 33), similar to that observed in Cdk5$^{-/-}$ muscles. The similarity in the NMJ phenotypes between the NRG/ErbB-mutant mice and Cdk5-null mice is consistent with our previous demonstration that Cdk5 activity is essential for the activation of NRG/ErbB signaling at the NMJ. We show, in this study, that Cdk5 regulates the tyrosine phosphorylation of both ErbB2/3 receptors, in addition to modulating ErbB2 kinase activity *in vivo* (Fig. 1) (5, 25). Despite the attenuation of ErbB-receptor activation in Cdk5$^{-/-}$ muscle, AChR

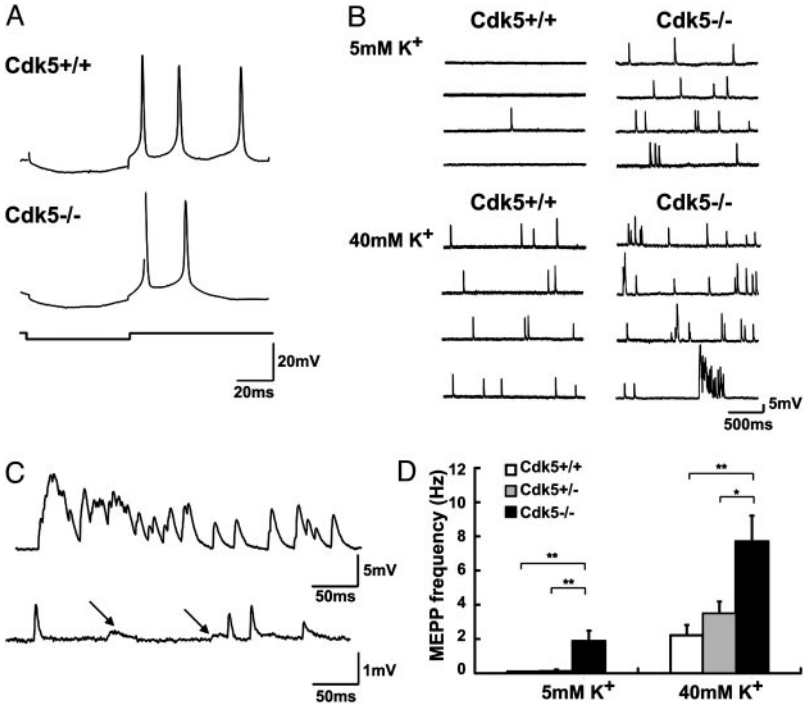

Fig. 5. Cdk5$^{-/-}$ embryos exhibited higher frequencies of MEPPs. Typical responses of Cdk5$^{+/+}$ and Cdk5$^{-/-}$ muscles to intracellular current injection (*A*) and recordings of MEPP frequencies under low (*Upper*) and high (*Lower*) K$^+$ concentration (*B*). (*C*) (*Upper*) Synchronous bursts of MEPPs, resulting in big depolarizing potentials, were often seen in the Cdk5$^{-/-}$ muscles under high K concentration. (*Lower*) a Cdk5$^{-/-}$ muscle had two types of MEPPs, fast and slow, (indicated by arrows). The slow MEPPs also had smaller amplitudes, consistent with an origin of far electrotonic distance. (*D*) Pooled data, showing that Cdk5$^{-/-}$ muscles had significantly higher MEPP frequencies, compared with that of Cdk5$^{+/+}$ and Cdk5$^{+/-}$ muscles. Cdk5$^{+/+}$ ($n = 17$ from 9 embryos); Cdk5$^{+/-}$ ($n = 16$ from 12 embryos); Cdk5$^{-/-}$ ($n = 16$ from 9 embryos). *, $P < 0.05$; **, $P < 0.01$, by one-way ANOVA followed by Tukey test.

subunit transcription remains relatively unchanged, in contrast to our previous demonstration that Cdk5 is required for NRG/ErbB-mediated regulation of AChR subunit transcription in myotube culture (5). The differential effects of Cdk5/NRG signaling on AChR transcription *in vitro* and *in vivo* might be due to the presence of redundant signaling mechanism in muscle, i.e., agrin/MuSK (16, 34, 35).

In this study, we have identified an unexpected role of Cdk5 in agrin-induced clustering of AChRs. Although Cdk5-deficient myotube culture remains responsive to agrin, the sizes of AChR clusters are larger. Similar observations of larger PSD-95 and channel receptor clusters were evident in central synapses of Cdk5-deficient cortical neurons (8). This finding supports the possibility that Cdk5 regulates the clustering of channel receptors at both central and peripheral synapses. During the formation of NMJ, AChR clusters are initially assembled into microclusters, followed by condensation and formation of large clusters. Cdk5 may thus regulate the size of AChR clusters through the regulation of formation and/or stabilization of AChR clusters.

How may Cdk5 regulate the formation or stabilization of AChR clusters? To a large extent, the initial clustering of AChRs at the NMJ is mediated by agrin/MuSK signaling (36). Because MuSK fails to associate with Cdk5/p35 (5) and does not contain optimal consensus sequences for Cdk5, the effect of Cdk5 on AChR clustering observed in this study is likely not mediated by a direct effect on MuSK but, rather, by modulating downstream signals. Binding of agrin to the MuSK receptor complex, for example, leads to the activation of Rac and Pak (26, 37). Because Cdk5 has been shown to phosphorylate Pak and RhoGEF, which could activate Rho activity (38, 39), Cdk5 may directly or indirectly impact on the clustering of AChRs. The detailed mechanism underlying the effect of Cdk5 on this aspect of postsynaptic specialization remains to be elucidated. Alternatively, Cdk5 may affect the disassembly of AChR clusters. NRG/ErbB activation was suggested to decrease the agrin-induced AChR clusters by increasing the rate of AChR disassembly (40). It is, therefore, possible that attenuation of ErbB-receptor activation in Cdk5-deficient myotubes or mutant muscle regulates the AChR clustering.

Upon stimulation of phrenic nerves, mutant diaphragms respond with a massive contraction, indicating that the AChR endplates are functional in $Cdk5^{-/-}$ embryos. The increase in MEPP frequency observed in $Cdk5^{-/-}$ muscle suggests an increase of spontaneous ACh release at the presynaptic terminals, implicating an enhanced synaptic transmission at the NMJ of $Cdk5^{-/-}$ mice. This observation is consistent with the suggested functions of Cdk5 in neurotransmitter release previously proposed, because Cdk5 has been identified to phosphorylate various substrates at nerve terminals that are involved in vesicle exocytosis, endocytosis, and recycling (41–43). Although the molecular mechanism underlying the regulation of the transmitter release by Cdk5 is unclear, here we demonstrate that absence of Cdk5 promotes the transmitter release at peripheral synapses *in vivo*.

In summary, Cdk5 deficiency leads to aberrant pre- and postsynaptic development of the NMJ and defects in intracellular signaling in muscle. Although Cdk5 activity is prominently detected in neurons, we have shown that the defects at the NMJs are, at least in part, contributed by Cdk5 activity in Schwann cells or postsynaptic muscle. The NMJ phenotype observed in the $Cdk5^{-/-}$ embryos highlights the potential importance of this kinase in orchestrating diverse signals to direct synapse formation. Although Cdk5 functions at the NMJ are just beginning to be explored, our data demonstrate the essential role of Cdk5-mediated signaling in the development of peripheral synapses and reveal the unexpected involvement of Cdk5 in regulating the clustering of AChRs. Further studies to decipher the functions of Cdk5 through the identification of Cdk5 substrates in muscle will lead to additional insights into the molecular mechanisms underlying synapse formation. Generation of conditional knockout mice that lack Cdk5 expression in motor nerve or muscle, for example, will also provide insights into molecular mechanisms that underlie the abnormal phenotypes observed.

We thank Drs. Ashok Kulkarni (National Institutes of Health, Bethesda) and Tom Curran (St. Jude Children's Research Hospital, Memphis, TN) for Cdk5-null mice, Dr. Shin-ichi Hisanaga (Tokyo Metropolitan University, Tokyo) for recombinant Cdk5/p35 protein, Dr. Zelda Cheung for helpful comments on the manuscript, and members of the Ip laboratory for helpful discussions. The expert technical assistance of Winnie W. Y. Chien, Pui Shan Au, Alberto Ng, and Yu Chen is also gratefully acknowledged. This work was supported by the Research Grants Council of Hong Kong (HKUST6091/01M, 6119/04M and HKUST 3/03C), the Area of Excellence Scheme of the University Grants Committee (AoE/B-15/01), and the Hong Kong Jockey Club. N.Y.I. is a Croucher Foundation Senior Research Fellow.

1. Dhavan, R. & Tsai, L. H. (2001) *Nat. Rev. Mol. Cell Biol.* **2**749–759.,
2. Ohshima, T., Ward, J. M., Huh, C. G., Longenecker, G., Veeranna, Pant, H. C., Brady, R. O., Martin, L. J. & Kulkarni, A. B. (1996) *Proc. Natl. Acad. Sci. USA* **93,** 11173–11178.
3. Chae, T., Kwon, Y. T., Bronson, R., Dikkes, P., Li, E. & Tsai, L. H. (1997) *Neuron* **18,** 29–42.
4. Kwon, Y. T., Tsai, L. H. & Crandall, J. E. (1999) *J. Comp. Neurol.* **415,** 218–229.
5. Fu, A. K., Fu, W. Y., Cheung, J., Tsim, K. W., Ip, F. C., Wang, J. H. & Ip, N. Y. (2001) *Nat. Neurosci.* **4,** 374–381.
6. Li, B. S., Sun, M. K., Zhang, L., Takahashi, S., Ma, W., Vinade, L., Kulkarni, A. B., Brady, R. O. & Pant, H. C. (2001) *Proc. Natl. Acad. Sci. USA* **98,** 12742–12747.
7. Cheng, K. & Ip, N. Y. (2003) *Neurosignals* **12,** 180–190.
8. Morabito, M. A., Sheng, M. & Tsai, L. H. (2004) *J. Neurosci.* **24,** 865–876.
9. Sanes, J. R. & Lichtman, J. W. (1999) *Annu. Rev. Neurosci.* **22,** 389–442.
10. Sanes, J. R. & Lichtman, J. W. (2001) *Nat. Rev. Neurosci.* **2,** 791–805.
11. Luo, Z., Wang, Q., Dobbins, G. C., Levy, S., Xiong, W. C. & Mei, L. (2003) *J. Neurocytol.* **32,** 697–708.
12. Fischbach, G. D. & Rosen, K. M. (1997) *Annu. Rev. Neurosci.* **20,** 429–458.
13. Buonanno, A. & Fischbach, G. D. (2001) *Curr. Opin. Neurobiol.* **11,** 287–296.
14. Falls, D. L. (2003) *J. Neurocytol.* **32,** 619–647.
15. Lin, W., Sanchez, H. B., Deerinck, T., Morris, J. K., Ellisman, M. & Lee, K. F. (2000) *Proc. Natl. Acad. Sci. USA* **97,** 1299–1304.
16. Yang, X., Arber, S., William, C., Li, L., Tanabe, Y., Jessell, T. M., Birchmeier, C. & Burden, S. J. (2001) *Neuron* **30,** 399–410.
17. Greer, J. J., Allan, D. W., Martin-Caraballo, M. & Lemke, R. P. (1999) *J. Appl. Physiol.* **86,** 779–786.
18. Vartanian, T., Goodearl, A., Viehover, A. & Fischbach, G. (1997) *J. Cell Biol.* **137,** 211–220.
19. Cheng, L., Esch, F. S., Marchionni, M. A. & Mudge, A. W. (1998) *Mol. Cell. Neurosci.* **12,** 141–156.
20. Fu, A. K., Cheung, W. M., Ip, F. C. & Ip, N. Y. (1999) *Mol. Cell. Neurosci.* **14,** 241–253.
21. Conlon, R. A. (1997) *Methods Mol. Biol.* **63,** 257–262.
22. Fu, A. K., Smith, F. D., Zhou, H., Chu, A. H., Tsim, K. W., Peng, B. H. & Ip, N. Y. (1999) *Eur. J. Neurosci.* **11,** 373–382.
23. Fu, W. Y., Fu, A. K., Lok, K. C., Ip, F. C. & Ip, N. Y. (2002) *NeuroReport* **13,** 243–247.
24. Misgeld, T., Burgess, R. W., Lewis, R. M., Cunningham, J. M., Lichtman, J. W. & Sanes, J. R. (2002) *Neuron* **36,** 635–648.
25. Li, B. S., Ma, W., Jaffe, H., Zheng, Y., Takahashi, S., Zhang, L., Kulkarni, A. B. & Pant, H. C. (2003) *J. Biol. Chem.* **278,** 35702–35709.
26. Weston, C., Yee, B., Hod, E. & Prives, J. (2000) *J. Cell Biol.* **150,** 205–212.
27. Dai, Z., Luo, X., Xie, H. & Peng, H. B. (2000) *J. Cell Biol.* **150,** 1321–1334.
28. Jessen, K. R. & Mirsky, R. (1998) *Microsc. Res. Tech.* **41,** 393–402.
29. Maurel, P. & Salzer, J. L. (2000) *J. Neurosci.* **20,** 4635–4645.
30. Li, Y., Tennekoon, G. I., Birnbaum, M., Marchionni, M. A. & Rutkowski, J. L. (2001) *Mol. Cell. Neurosci.* **17,** 761–767.
31. Trinidad, J. C., Fischbach, G. D. & Cohen, J. B. (2000) *J. Neurosci.* **20,** 8762–8770.
32. Morris, J. K., Lin, W., Hauser, C., Marchuk, Y., Getman, D. & Lee, K. F. (1999) *Neuron* **23,** 273–283.
33. Wolpowitz, D., Mason, T. B., Dietrich, P., Mendelsohn, M., Talmage, D. A. & Role, L. W. (2000) *Neuron* **25,** 79–91.
34. Lin, W., Burgess, R. W., Dominguez, B., Pfaff, S. L., Sanes, J. R. & Lee, K. F. (2001) *Nature* **410,** 1057–1064.
35. Escher, P., Lacazette, E., Courtet, M., Blindenbacher, A., Landmann, L., Bezakova, G., Lloyd, K. C., Mueller, U. & Brenner, H. R. (2005) *Science* **308,** 1920–1923.
36. DeChiara, T. M., Bowen, D. C., Valenzuela, D. M., Simmons, M. V., Poueymirou, W. T., Thomas, S., Kinetz, E., Compton, D. L., Rojas, E., Park, J. S., *et al.* (1996) *Cell* **85,** 501–512.
37. Luo, Z. G., Wang, Q., Zhou, J. Z., Wang, J., Luo, Z., Liu, M., He, X., Wynshaw-Boris, A., Xiong, W. C., Lu, B. & Mei, L. (2002) *Neuron* **35,** 489–505.
38. Nikolic, M., Chou, M. M., Lu, W., Mayer, B. J. & Tsai, L. H. (1998) *Nature* **395,** 194–198.
39. Xin, X., Ferraro, F., Back, N., Eipper, B. A. & Mains, R. E. (2004) *J. Cell Sci.* **117,** 4739–4748.
40. Trinidad, J. C. & Cohen, J. B. (2004) *J. Biol. Chem.* **279,** 31622–31628.
41. Nguyen, C. & Bibb, J. A. (2003) *J. Cell Biol.* **163,** 697–699.
42. Lee, S. Y., Wenk, M. R., Kim, Y., Nairn, A. C. & De Camilli, P. (2004) *Proc. Natl. Acad. Sci. USA* **101,** 546–551.
43. Tomizawa, K., Ohta, J., Matsushita, M., Moriwaki, A., Li, S. T., Takei, K. & Matsui, H. (2002) *J. Neurosci.* **22,** 2590–2597.